Hyperfine Interact (2009) 193:39–45
DOI 10.1007/s10751-009-0067-9

Observation of πK-atoms with DIRAC-II

Y. Allkofer (on behalf of the DIRAC-II collaboration)

Published online: 27 August 2009

Abstract We present evidence for the first observation of electromagnetically bound $\pi^{\pm}K^{\mp}$-pairs (πK-atoms) with the DIRAC-II experiment at the CERN-PS. The πK-atoms are produced by the 24 GeV/c proton beam in a thin Pt-target and the dissociated $\pi^{\pm}$ and $K^{\mp}$-mesons analyzed in a two-arm magnetic spectrometer. The observed enhancement at low relative momentum corresponds to the production of 173 ± 54 πK-atoms. The mean life of πK-atoms is related to the s-wave πK-scattering lengths. From these first data we derive a lower limit for the mean life of 1.5 fs at 84% confidence level.

Keywords DIRAC experiment · Exotic atoms · Scattering length · Chiral perturbation · QCD

PACS 36.10.-k · 32.70.Cs · 25.80.Nv · 29.30.Aj

1 Introduction

The study of electromagnetically bound hadronic pairs is an excellent method to probe QCD at very low energy. Opposite charge long-lived hadrons such as pions and kaons can form hydrogen-like atoms bound by the Coulomb interaction. The strong interaction introduces an additional repulsion or attraction, hence an energy shift of the atomic levels, in particular of the 1s-state. On the other hand, the mean life of the atom is related to the broadening of the width of the 1s-state.

Pion-pion interaction at low energy, strongly constrained by the approximate 2-flavour SU(2) (u,d) chiral symmetry, is the simplest and well understood hadron-hadron process [1, 2]. The observation of $\pi^{+}\pi^{-}$-atoms and a measurement of their mean life was reported in ref. [3].

Y. Allkofer (✉)
University of Zurich, 8057, Zürich, Switzerland
e-mail: yves.allkofer@cern.ch

The low energy interaction between the pion and the heavier (strange) kaon is a tool to study the more general 3-flavour SU(3) (u,d,s) structure of hadronic interaction at low energy which is not accessible in $\pi\pi$-interactions. A detailed study of πK-interaction provides insights into a potential flavour (u,d,s) dependence of the crucial order parameter or quark condensate in Chiral Perturbation Theory (ChPT) [4].

A measurement of the πK-atoms lifetime was proposed already in 1969 [5, 6] to determine the difference $|a_{1/2} - a_{3/2}|$ of the s-wave πK-scattering lengths, where the indices 1/2 and 3/2 refer to the isospin of the πK-system. The πK-atoms decay predominantly by strong interaction into the neutral meson pairs $\pi^0 K^0$. The decay width of πK-atoms in the ground state is given by the relation [5–7]:

$$\Gamma(A_{\pi K}) = \frac{1}{\tau_{1S}} = 8\,\alpha^3\,\mu_+^2\,p^*\,|a_{1/2} - a_{3/2}|^2\,(1+\delta). \tag{1}$$

τ_{1S} is the lifetime of πK-atoms in the ground state, α the fine structure constant, μ_+ the reduced mass and $p^* = 11.8$ MeV/c the outgoing K^0 or π^0 3-momentum in the πK center-of-mass system. The term $\delta \simeq 4\%$ [7] accounts for corrections. Hence, a measurement of $\Gamma(A_{\pi K})$ provides a value for the scattering length $|a_{1/2} - a_{3/2}|$. The mean life of πK-atoms is predicted to be 3.7 ± 0.4 fs [7].

The method used by DIRAC is to produce pions and kaons with a high energy proton beam impinging on a thin target. Pairs of oppositely charged mesons may interact and even form electromagnetically bound systems. Their subsequent ionization in the production target leads to mesons emerging from the target with low relative momentum. The mean life of the atoms can then be calculated from the number of observed low-momentum pairs. This method was first proposed in 1985 [8] and was successfully applied to $\pi^+\pi^-$-atoms (measurement of $A_{2\pi}$) in Serpukhov on the U-70 synchrotron internal proton beam [3, 9], and with DIRAC-I at the CERN-PS on beam line T8 [3]. Data from DIRAC-I lead to a mean life $\tau_{2\pi} = (2.91 \pm^{0.49}_{0.62})$ fs for $\pi^+\pi^-$-atoms [3].

In this paper we report on the search for πK-atoms and discuss the prospects to measure their mean life with the DIRAC-II apparatus.

2 Experimental setup

Details on the initial (DIRAC-I) apparatus used to study $\pi^+\pi^-$-atoms can be found in [10].

We now describe in more details the upgrade which was performed to search for and study πK-atoms [11]. The aperture of the detectors downstream of the dipole magnet was increased. The readout electronics for the upstream detectors and for some of the downstream detectors was modified to improve the resolution and the data collection efficiency. The upstream detectors (4–6), see Fig. 1, were either replaced or upgraded. However, they were not yet fully operational during data taking, and were therefore not used for the analysis presented here. The tracking is performed by the drift chambers (10) which have a spacial resolution of 90 μm. The vertical (11) and horizontal hodoscope consisting with a time resolution around 100 ps is used for timing. The N_2-Čerenkov detector (15) was already used previously to reject electrons and positrons. The inner part of the original container had to be

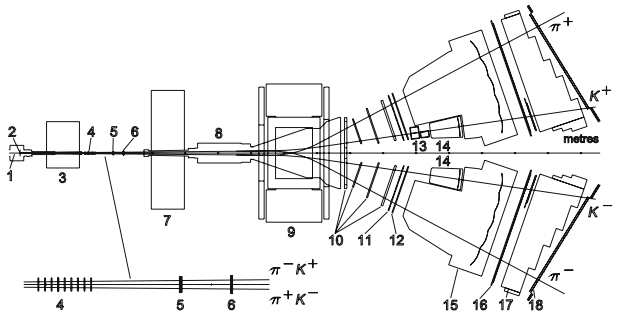

Fig. 1 Sketch of the DIRAC-II spectrometer (*top view*). *1* – proton beam, *2* – target, *3* – shield, *4* – microdrift chambers, *5* – scintillation fiber detector, *6* – ionization hodoscope, *7* – shield, *8* – vacuum chambers, *9* – dipole magnet, *10* – drift chambers, *11* – vertical hodoscopes, *12* – horizontal hodoscopes, *13* – aerogel Čerenkov modules, *14* – heavy gas Čerenkov detectors, *15* – N_2-Čerenkov detectors, *16* – preshowers, *17* – absorbers, *18* – muon scintillation hodoscopes. The *solid lines* crossing the spectrometer arms correspond to typical $\pi^{\pm}$- and $K^{\mp}$-trajectories from the ionization of πK-atoms in the production target

cut to clear space for the two new Čerenkov detectors needed for kaon identification. Since the momenta of the two mesons originating from the breakup of the πK-atoms are very small in the center-of-mass system, they have similar velocities in the laboratory system, and hence kaons are less deflected than pions. Typical trajectories are shown in Fig. 1. The heavy gas C_4F_{10}-Čerenkov detectors [12] in both arms (14) identify pions but do not respond to kaons nor (anti)protons. The aerogel Čerenkov detector in the left arm identifies kaons and reject protons [13, 14]. Such a detector is required only in the left arm since the contamination from antiprotons in the right arm is small due to their low production rate. The detector consists of two modules of 12ℓ each with a refractive index of $n = 1.015$ to cover the relevant momentum range between 4 and 8 GeV/c. The preshower detector (16) provides additional electron/hadron separation and the iron absorber (17) and the array of scintillation counters (18) are used to suppress muons.

3 Data analysis

As mentioned already, only detectors downstream of the dipole magnet are used here for event reconstruction. The tracking is described in detail in [3, 15].

The variable of interest in the following analysis is the relative momentum Q of the $K^{\pm}\pi^{\mp}$-pairs in their center-of-mass systems. In the transverse plane, the resolution on the relative momentum Q_T (typically 3 MeV/c) is determined by multiple scattering in the upstream detectors, while the resolution on the longitudinal component Q_L (< 0.4 MeV/c) is not affected [15, 16]. For further analysis we use therefore only Q_L.

We have verified that the new hardware and software were able to reproduce the observation of $\pi^+\pi^-$-atoms. Details of the procedure for $\pi^+\pi^-$ atoms can be found in [3, 15] leading to the detection of 7098 ± 533 $\pi^+\pi^-$-atoms [15].

We now describe the analysis steps [15]: accidental pairs are first removed using the time information from the vertical hodoscopes. For prompt pairs the time

difference between the positive and negative spectrometer arm lies between −0.5 and 0.5 ns. Accidental pairs are also needed for the subsequent analysis and we select those pairs with a time difference between −12 and −6 ns. The choice of the negative sign avoids the contamination from slow protons. Both event types have then to satisfy the following criteria:

- no electrons, positrons nor muons,
- $|Q_L| < 20$ MeV/c and $Q_T < 8$ MeV/c,
- the momentum of the kaon (pion) lies between 4 (1.2) GeV/c and 8 (2.1) GeV/c.

With the excellent time resolution of the vertical hodoscope pions, kaons and protons below 2.5 GeV/c can be separated by time-of-flight [17]. For the $\pi^- K^+$ analysis the TDC of the aerogel detector is used in addition to remove protons in the positive arm, while for the $\pi^+ K^-$ analysis, the time difference between the negative and the positive arm measured with the vertical hodoscope has to be negative in order to remove protons faking pions. Once the accidentals have been subtracted the prompt pairs (N^{pr} events) are composed of the following three types: ionized atomic-pairs (n^A events), Coulomb correlated pairs (N^C events) which are asymptotically unbound in contrast to atoms, and non-Coulomb-pairs (N^{nC} events) without Coulomb interactions in the final state. Therefore

$$N^{pr} = n^A + N^C + N^{nC}. \tag{2}$$

However, the background arising from $\pi^+\pi^-$- and $\pi^- p$-pairs with misidentified particles must be considered since the kaon flux is much lower than the pion and proton fluxes. We assume [15] that the background due to Coulomb uncorrelated pairs can be described with the Q_L-distribution of accidentals, following a similar analysis for $\pi^+\pi^-$-atoms [3]. On the other hand, Coulomb correlated pairs will be described by Monte-Carlo simulation [18, 19].

To determine the contribution from Coulomb- and non-Coulomb pairs we select the momentum range $3 < |Q_L| < 20$ MeV/c, where no atoms are expected. One can then write

$$\frac{dN^{pr}}{dQ_L} = \beta \cdot \frac{dN^C}{dQ_L} + (N^{pr} - \beta) \cdot \frac{dN^{acc}}{dQ_L}, \tag{3}$$

where $\frac{dN^C}{dQ_L}$ and $\frac{dN^{acc}}{dQ_L}$ are the (normalized) differential probabilities for Coulomb correlated or uncorrelated pairs, respectively. The fit variable β is the corresponding number of correlated pairs. We choose a bin size of 0.25 MeV/c. The χ^2-function to be minimized is

$$\chi^2 = \sum_{|i|=13}^{80} \left[\frac{\frac{dN^{pr}}{dQ_{L,i}} - \beta \cdot \frac{dN^C}{dQ_{L,i}} - (N^{pr} - \beta) \cdot \frac{dN^{acc}}{dQ_{L,i}}}{\sigma_i^{pr}} \right]^2, \tag{4}$$

where σ_i^{pr} are the corresponding statistical errors in the measured number of prompt pairs. Figure 2a shows the MINUIT results for Coulomb- and non-Coulomb contributions to $\pi^- K^+$ events. Since the shapes of both contributions are known, one can extrapolate into the $|Q_L| < 3$ MeV/c signal region. The difference (residuals) between the data and the sum of both contributions is plotted in Fig. 2b. Above $|Q_L| = 3$ MeV/c the residuals are consistent with zero, while the enhancement at low relative momentum is the first evidence for $\pi^- K^+$-atoms.

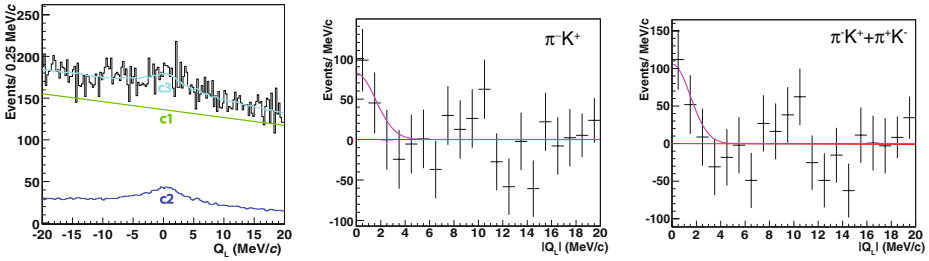

Fig. 2 **a** Q_L-distribution for the $\pi^- K^+$ data sample (26 μm Pt-target). The histogram shows the data. The fitted background (*c3*) is the sum of non-Coulomb (*c1*) and Coulomb (*c2*) contributions. In **b** and **c** are plotted the residuals between data and fitted background for the $\pi^- K^+$ and $\pi^- K^+ + \pi^+ K^-$ data samples, respectively. The *solid lines* illustrate the distribution of atomic-pairs (see text)

A Gaussian distribution describes adequately the low momentum enhancement observed in the $\pi^+\pi^-$-data [15]. Accordingly, a Gaussian distribution can also be applied here (line in Fig. 2) to illustrate the Q_L-distribution from πK-atoms. This leads to the observation of 139 ± 67 atomic $\pi^- K^+$-pairs.

A similar fit is applied to $\pi^+ K^-$ events. However, the number of events is much smaller, mainly due to the much lower production cross section for negative kaons. The fit results are summarized in Table 1. The errors on the number of Coulomb-pairs β are the full (MINOS) errors, while the errors on n^A are given by the square roots of the bin contents, statistical fluctuations on the much larger Monte-Carlo sample being negligible.

Figure 2c shows the sum of the $\pi^- K^+$ and $\pi^+ K^-$ residuals. We obtain

$$A_{\pi^\pm K^\mp} = 173 \pm 54 \tag{5}$$

detected atomic pairs.

The significance of 3.2 σ is not very high. However, the evidence for the observation of πK-atoms is strengthened by the observation of correlated Coulomb-pairs which, a fortiori, implies that atoms have also been produced. This can be seen as follows: non-Coulomb pairs have the same Q_L-distribution as accidentals. Hence dividing the distribution for prompt pairs by the one for accidentals one obtains the correlation function R describing Coulomb-pairs. The function R, shown in Fig. 3a for $\pi^- K^+$ as a function of $|Q_L|$, is clearly not consistent with unity and therefore proves that Coulomb-pairs have been observed.

In the signal region ($|Q_L| < 3$ MeV/c) one obtains for the data in Fig. 3a $N^C = 858 \pm 247$ Coulomb-pairs from data only (without resorting to Monte-Carlo). The same procedure can be applied to $\pi^+ K^-$ events, leading to $N^C = 313 \pm 148$ Coulomb-pairs. The ratio k of the total number of produced atoms to the total number of Coulomb-pairs has been calculated: $k = 0.615$ [20]. However, one needs to take into account the acceptance of the apparatus and the cuts applied in the analysis. By Monte Carlo simulation we determine the ratio $k_{exp} = 0.231$ between the number N^A of atoms produced within acceptance and the number N^C of detected Coulomb-pairs below $|Q_L| = 3$ MeV/c. This then leads to $N^A = 198 \pm 57$ $\pi^- K^+$- and 72 ± 34 $\pi^+ K^-$-atoms (Table 1, right).

Table 1 Left: number of Coulomb-pairs β and detected atomic-pairs n^A from the χ^2-minimization

Atom	χ^2-minimization			Direct Coulomb measurement	
	χ^2/ndof	β	n^A	N^A	n_e^A
$\pi^- K^+$	122/130	$4'215 \pm 1'008$	143 ± 53	198 ± 57	104 ± 30
$\pi^+ K^-$	164/130	$1'356 \pm 396$	29 ± 15	72 ± 34	38 ± 18

Right: expected number of atoms N^A calculated from the number of detected Coulomb-pairs, and expected number of atomic pairs n_e^A using a breakup probability of 53%

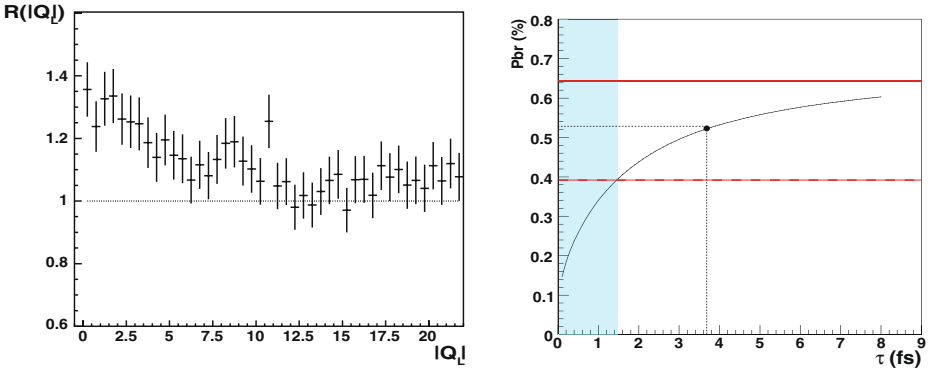

(a) (b)

Fig. 3 **a** Correlation R as a function of $|Q_L|$ for $\pi^- K^+$-pairs. The deviation for low $|Q_L|$ from the *horizontal dotted line* proves the existence of Coulomb correlated $\pi^- K^+$-pairs. **b** Breakup probability P_{br} for the 28 μm Pt-target as a function of mean life for πK-atoms in 1s-state. The *horizontal solid line* is the measured breakup probability and the *horizontal dashed line* its 1σ lower bound. The *shaded area* is excluded with a confidence level of 84%. The *horizontal dotted line* shows the theoretical prediction according to [7]

The breakup probability

$$P_{br} = \frac{n^A}{N^A} \tag{6}$$

relates the number of atoms to the number of atomic pairs. A calculation of the breakup probability as a function of mean life (Fig. 3b) has been performed using the Born approximation [15]. For the predicted mean life of 3.7 ± 0.4 fs [7] the corresponding breakup probability P_{br} is 53% (dotted lines in Fig. 3b). From Eq. 6 we then find the number n_e^A of expected pairs given in Table 1, right. These numbers are in good agreement with the number n^A of atomic-pairs obtained from the χ^2 minimization (fourth column).

Conversely, we use the number of atomic-pairs n^A from the χ^2 minimization (Table 1) and the number of Coulomb-pairs below $|Q_L| < 3$ MeV/c to calculate the breakup probability P_{br} from Eq. 6 with $N^A = k_{exp} \cdot N^C$. The result $P_{br} = 64 \pm 25\%$ is shown by the solid red line in Fig. 3b. This leads to a lower limit for the mean life of πK-atoms of $\tau_{1S} \geq 1.5$ fs at a confidence level of 84% [21].

References

1. Weinberg, S.: Phys. Rev. Lett. **17**, 616 (1966)
2. Colangelo, G., Gasser, J., Leutwyler, H.: Nucl. Phys. **B603**, 125 (2001)
3. Adeva, B., et al.: Phys. Lett., B **619**, 50 (2005)
4. Descotes-Genon, S., Girlanda, L., Stern, J.: JHEP **0001**, 041 (2000); Eur. Phys. J. **C27**, 115 (2003)
5. Bilen'kii, S.M., van Hieu, N., Nemenov, L.L., Tkebuchava, F.G.: Yad. Fiz. **10**, 812 (1969)
6. Bilen'kii, S.M., van Hieu, N., Nemenov, L.L., Tkebuchava, F.G.: Sov. J. Nucl. Phys. **10**, 469 (1969)
7. Schweizer, J.: Phys. Lett., B **587**, 33 (2004)
8. Nemenov, L.L.: Yad. Fiz. **41**, 980 (1985); Sov. J. Nucl. Phys. **41**, 629 (1985)
9. Afanasyev, L., et al.: Phys. Lett., B **338**, 478 (1994)
10. Adeva, B., et al.: Nucl. Instr. Meth. A **515**, 467 (2003)
11. Adeva, B., et al.: Addendum to the DIRAC Proposal. CERN-SPSC-2004-009, SPSC-P-284 Add.4
12. Kuptsov, A.: DIRAC note 08-01. http://dirac.web.cern.ch/DIRAC/i_notes.html
13. Allkofer, Y., et al.: Nucl. Instr. Meth. A **582**, 497 (2007)
14. Allkofer, Y., et al.: Nucl. Instr. Meth. A **595**, 84 (2008)
15. Allkofer, Y.: Ph.D. thesis, Universität Zürich (2008)
16. Allkofer, Y., Benelli, A., Tauscher, L.: DIRAC note 07-08. http://dirac.web.cern.ch/DIRAC/i_notes.html
17. Adeva, B., et al.: Nucl. Instr. Meth. A **491**, 41 (2002)
18. Sakharov, A.D.: Zh. Eksp. Teor. Fiz. **18**, 631 (1948)
19. Lednicky, R.; Prep. arXiv:nucl-th/0501065
20. Afanasyev, L., Voskresenskaya, O.: Phys. Lett. B **453**, 302 (1999)
21. Allkofer, Y., et al.: Phys. Lett. B **674**, 11–16 (2009)